Journal of the Korean Institute of Illuminating and Electrical Installation Engineers (2014) 28(12) : 95~102
http://dx.doi.org/10.5207/JIEIE.2014.28.12.095 ISSN 1229-4691(Print) ISSN 2287-5034(Online)

논문 28-12-13

Coordinated Control of an Independent Multi-phase Permanent Magnet-type Transverse Flux Linear Machine Based on Magnetic Levitation

Seon-Hwan Hwang* · Soon-Kurl Kwon · Young-Gi Hwang · Deok-Je Bang**

Abstract

This paper proposes a coordinated control for an independent multi-phase transverse flux linear synchronous motor (IM-TFLSM) based on magnetic levitation. The stator structures of the IM-TFLSM are composed of a two set, which has independent three-phase windings and a double-sided air-gap as opposed to the conventional Y-connected three-phase linear motors. A suitable control algorithm is necessary to operate the applied linear machine. This study proposes a coordinated control algorithm for adjusting the mover air-gap and thrust force of the IM-TFLSM in order to maintain air-gap and phase shifted current control of the independent 3-phase modules. In addition, the principle of operation and its special structures are described in detail and the validity and effectiveness of the control algorithm is verified through multiple experimental results.

Key Words : Independent Multi-phase Permanent Magnet-type Transverse Flux Linear Synchronous Motor, Magnetic Levitation, Phase Shifted Current Control, Coordinated Control

1. Introduction

Recently, linear motor drives have been widely used in various industrial applications such as automatic systems, machine tool positioning, and transportation systems. When driving the transportation system, the linear motor drives need to develop not only a contactless levitation system but also a contact-free propulsion system. Linear motors produce a high normal force compared to the thrust force developed by the motor itself [1-3]. In addition, the use of a magnetic levitation system is steadily increasing in high-speed motor drives, for generators like a flywheel drive, in medical equipment, and for harsh environments such as high or low temperature and vacuums. The magnetic levitation drive offers many advantages, such as high velocity, zero wear, and zero maintenance, allowing it to provide high reliability.

* Main author : Dept. of Electrical Eng., Kyungnam Univ., Korea
** Corresponding author : Electric Motor Research Center, Electric Propulsion Research Division, KERI, Korea
Tel : +82-55-280-1487, Fax : +82-55-280-1216
E-mail : djbang@keri.re.kr
Date of submit : 2014. 10. 1
First assessment : 2014. 10. 7
Completion of assessment : 2014. 11. 3

In this paper, a coordinated control algorithm for an independent multi-phase transverse flux linear synchronous motor (IM-TFLSM) is proposed. The magnetic levitation and thrust force are adjusted only by the use of each stator winding without any additional windings and power converters to control air-gap length. The feasibility and effectiveness of the proposed control system are shown by the experimental results on the prototype independent three-phase magnetic levitation transverse flux linear motor.

2. Description of Magnetic Levitation IM-TFLSM System and Control Algorithm

2.1 Configuration of IM-TFLSM

In order to control the air-gap based on the magnetic levitation and thrust force, an independent 3-phase transverse flux linear synchronous motor (IM-TFLSM) is shown in Fig. 1 [4-5]. The IM-TFLSM used is composed of multiple-module and multi-phase structures having separated magnetic and electric circuits per each phase. The stator winding of the IM-TFLSM consists of independent 3-phase modular and symmetric structures with the double-sided air-gap. Each stator phase windings are separated by 120 electrical degrees.

The area of the stator teeth is 480㎟. In addition, it can be seen that only the coils facing them over PMs will produce the magnetic levitation and the thrust force as shown in Fig. 1. The mover is also constructed with multiple-modules including PMs.

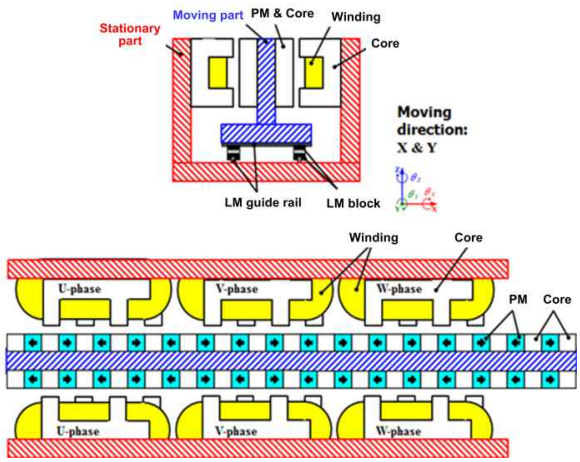

Fig. 1. Front and upper view of IM-TFLSM

2.2 Analysis Results of IM-TFLSM

Fig. 2 shows the analysis model including the coil current direction when the mover is moved. According to the mover position variation, the current direction in the each phase coil is changed in

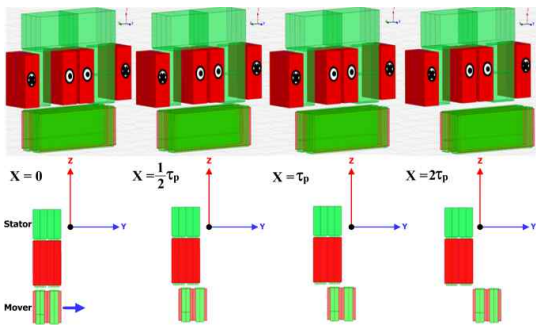

Fig. 2. Coil current direction under mover position

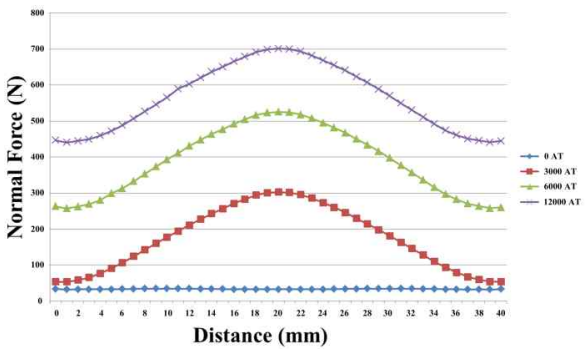

Fig. 3. Absolute normal force under mover position at 3mm air-gap

sequence.

As a result, the generated thrust and normal forces toward the x- and y-directions at 3mm air-gap are shown in Fig. 3 and Fig. 4.

From Fig. 3 and Fig. 4, each phase of the normal force and thrust force is displaced by 90 degree. Therefore, the IM-TFLSM can produce not only thrust force in the x-axis direction, but also normal force in the y-axis direction, respectively.

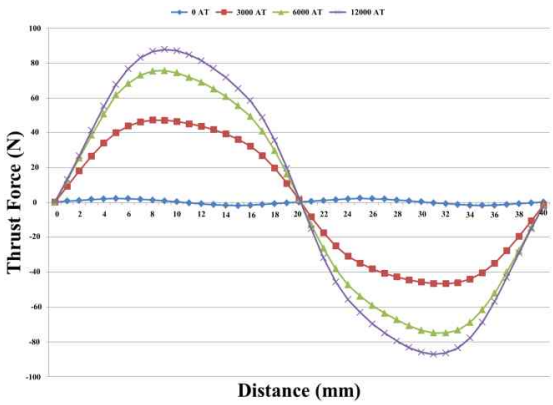

Fig. 4. Thrust force under mover position at 3mm air-gap

2.3 Mathematical Modeling of IM-TFLSM

The voltage equation based on the independent 3-phase IM-TFLSM can be expressed as [6-8]

$$v_j = R_j i_j + \frac{d\lambda_j}{dt} \quad , \quad j = a1, b1, c1 \tag{1}$$

where v_j is the j -phase stator voltage. R_j is the j -phase stator resistance. i_j is the j -phase stator current. λ_j is the flux linkage per j -phase.

The flux linkage of the j -phase in the independent 3-phase IM-TFLSM can be obtained by [6-8]

$$\lambda_j = \sum_{k=1}^{3} L_{jk} i_k + \lambda_{jf} \tag{2}$$

where λ_{jf} is the j -phase flux linkage according to the permanent magnetic. $L_{ik}(j=k)$ is the self inductance between j - or k -phase.. $L_{ik}(j \neq k)$ is the mutual inductance between j -and k -phase.

As shown in Fig. 1, there is no coupling effect between the magnetic circuit and electric circuits per each phase. Therefore, the flux linkage can be easily represented as:

$$\lambda_j = L_{jj} i_j + \lambda_{jf}, \quad j = a1, b1, c1 \tag{3}$$

where $L_{ik}(j \neq k)$ equals zero.

From Eq. (1), the voltage equation can be rewritten by

$$\begin{aligned} v_j &= R_j i_j + \frac{d\lambda_j}{dt} \\ &= R_j i_j + \frac{d}{dt}(L_{jj} i_j + \lambda_{jf}) \\ &= R_j i_j + \frac{dL_s}{dt} i_j + L_s \frac{di_j}{dt} + \frac{d\lambda_{jf}}{dt} \end{aligned} \tag{4}$$

where $L_{ik}(j=k)$ is L_s.

The voltage equation of IM-TFLSM, including the self inductance and the flux linkage variation of the mover PM, is shown in below.

$$\begin{aligned} v_j = R_j i_j &+ (L_s + \frac{\partial L_s}{\partial i_j} i_j)\frac{di_j}{dt} + (\frac{\partial L_s}{\partial x} i_j + \frac{\partial \lambda_{jf}}{\partial x})\frac{dx}{dt} \\ &+ (\frac{\partial L_s}{\partial y} i_j + \frac{\partial \lambda_{jf}}{\partial y})\frac{dy}{dt} \end{aligned} \tag{5}$$

where x is the mover position and y is the displacement of air-gap length.

Under a balanced electrical power condition, the thrust force and normal force related to the air-gap developed by the IM-TFLSM is:

$$F_x = \sum_{j=1}^{3}(\frac{1}{3}\frac{\partial L_s}{\partial x} i_j + \frac{\partial \lambda_{jf}}{\partial x})i_j \quad (6)$$

$$F_y = \sum_{j=1}^{3}(\frac{1}{3}\frac{\partial L_s}{\partial y} i_j + \frac{\partial \lambda_{jf}}{\partial y})i_j \quad (7)$$

The mechanical equation of IM-TFLSM can be represented as

$$F_x = M\frac{dv}{dt} + C_f v + F_L + F_y \quad (8)$$

where F_x is the thrust force. M is the total mass of the mover. F_L is the external load force. C_f is the friction coefficient. v is the mover speed. F_y is the normal force.

From (6), the thrust force F_x is the x-direction component shown in Fig. 1. The normal force that existed in IM-TFLSM F_y is the attractive force between the primary current and permanent magnet flux linkage crossing the air-gap.

As can be seen in (6) and (7), the thrust and normal forces are the functions of primary current, permanent magnet flux linkage and the phase angle between them. It is possible to simultaneously control the two forces by adjusting the primary voltage vector based on the phase angle.

2.4 Proposed Coordinated Current Control

The transfer function of the magnetic levitation system is not stable so that the controller must stabilize it by using a feedback loop. A proportional-integral-derivative (PID) controller is suitably used for magnetic levitation IM-TFLSM as shown below:

$$C(s) = K_p\left(1 + \frac{1}{T_i s} + \frac{T_d s}{1+\eta T_d s}\right) \quad (9)$$

where K_p is the proportional gain. η is the range of derivative coefficient. T_i is the integral time and T_d is the derivative time.

In order to control the air-gap and mover position, a stationary PI current regulator is applied. Each phase current command is summing the output of thrust force control and the output of normal force control as shown in Fig. 5.

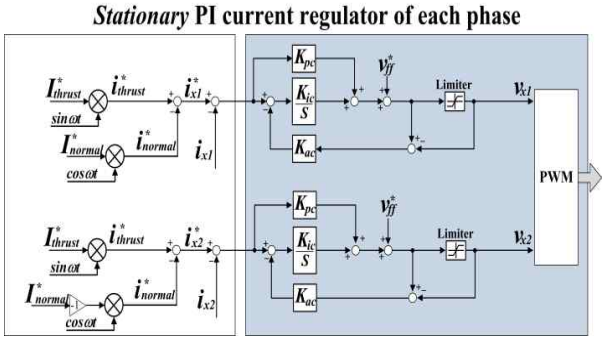

Fig. 5. Coordinated current regulators for thrust and normal force controls

Fig. 6 shows the control block diagram of the IM-TFLSM including magnetic levitation control and position control, respectively. The air-gap reference related to the normal force is produced by the PID controller. After operating the air-gap PID controller, the normal force current reference generator provides 90 degree phase shift current commands compared to the current reference of

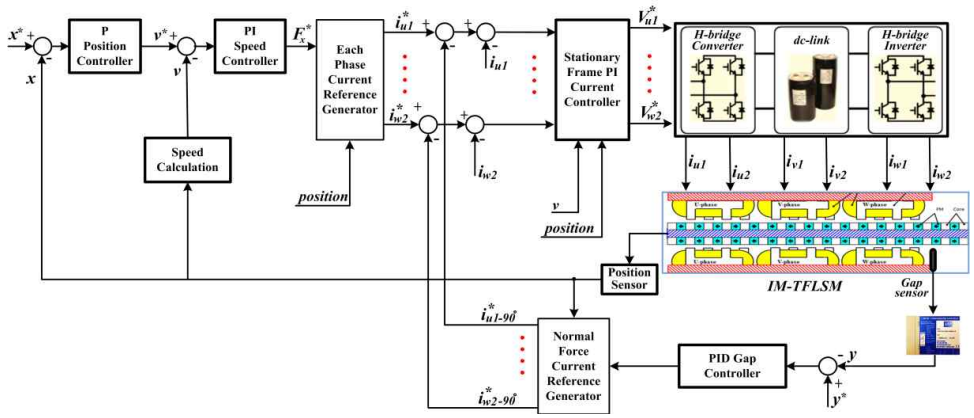

Fig. 6. Control block diagram of IM-TFLSM

position control. These signals are added in the outputs of the PI speed controller of the position control section. The final three-phase current commands are given to the stationary frame PI current regulator.

3. Experimental Results

The independent multi-phase transverse flux linear synchronous motor has been configured to show the effectiveness of the proposed magnetic levitation and the thrust force system. Fig. 7 shows the overall block diagram of the magnetic levitation IM-TFLSM drive system. In addition, the single-phase bi-directional AC/DC/AC converter modules are implemented by the IGBT modules with a switching frequency of 10kHz.

The control algorithm is performed by a digital signal processor (DSP) control system. The displacement sensor is installed at the stationary section. Fig. 8 represents the photo of the magnetic levitation IM-TFLSM, which includes single-phase power converters, a control board, and a displacement sensor. The detailed specifications of the applied IM-TFLSM are described in Table I.

Fig. 9 shows the experimental results of the IM-TFLSM drive system. At the standstill, the actual air-gap tracks well when the air-gap command is changed from 1.2mm to 3.5mm, as shown in Fig. 9. When running the air-gap control between 3.0mm and 2.5mm, as shown in Fig. 10, the real air-gap maintains control by using the proposed algorithm. In addition, dc currents are generated in each phase stator winding during standstill operation.

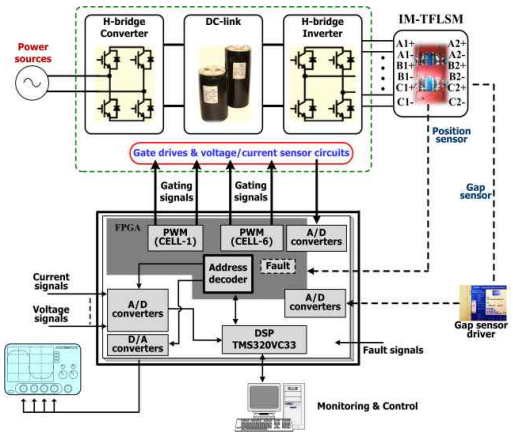

Fig. 7. Overall block diagram of IM-TFLSM drive system

Fig. 11 describes the experimental waveform under both air-gap and position control. Despite the position command variation from 0.01m to 0.15m,

the actual air-gap also tracks the air-gap command 3.0mm as shown in Fig. 11. As a result, the performance of the proposed coordinated current control method is verified.

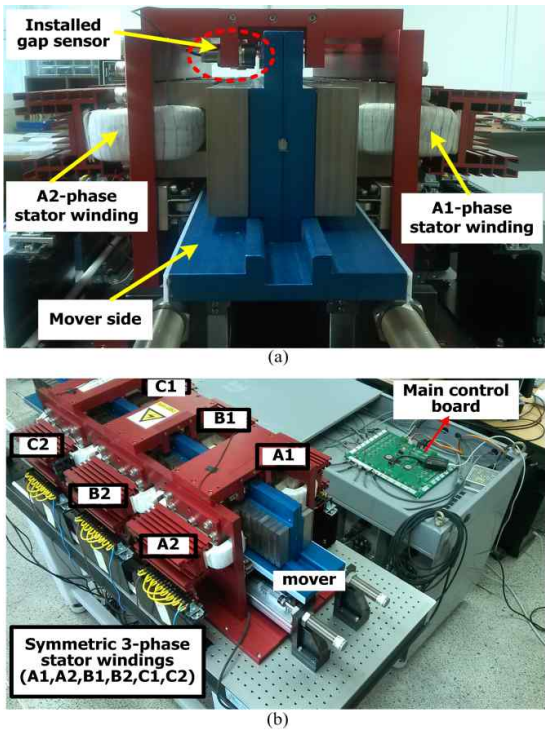

Fig. 8. Pictures of IM-TFLSM experimental setup. (a) Front view. (b) Upper view with a control board and power converters

Table 1. Specifications of IM-TFLSM drive system

System Parameters	Values
Driver model of displacement sensor	ECL101
Analog output of displacement sensor	0~10VDC
Range of displacement sensor	8mm
Target material of displacement sensor	1-6061 Al
Rated MMF of IM-TFLSM	6000AT
Rated thrust force of IM-TFLSM	250N 1-phase
Mover PM material of IM-TFLSM	Ferrite
Stator material of IM-TFLSM	S20c
Nominal air-gap length	3mm
Sampling period	100μs
Switching frequency	10kHz

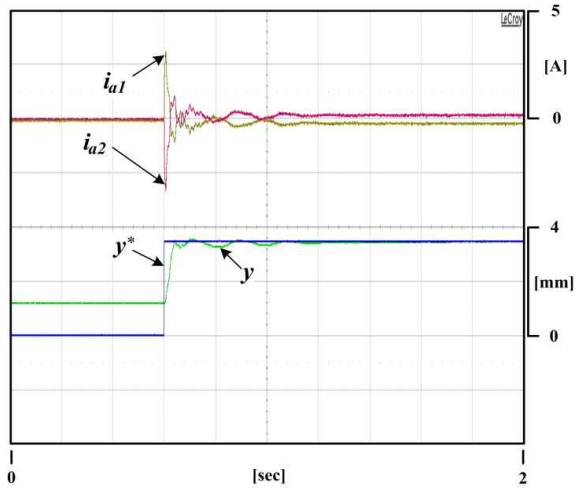

Fig. 9. Experimental waveform under air gap control and position control (standstill)

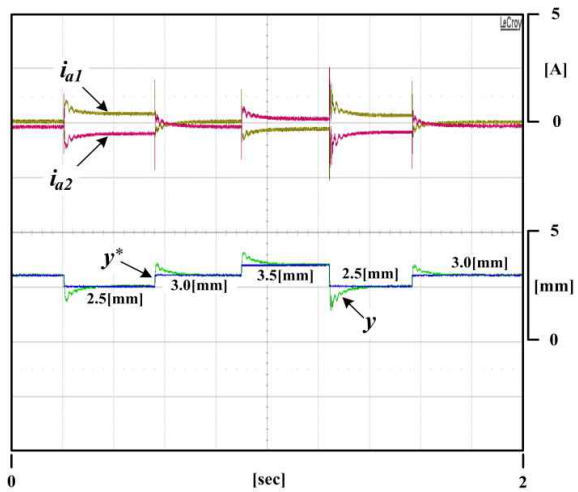

Fig. 10. Experimental waveform under air gap control and position control (standstill)

Fig. 12 shows the experimental results of the magnetic levitation drive system according to the position command variation between 0.05m and 0.2m. As shown in Fig. 12, when operating the position and magnetic levitation controls, the real air gap follows the air gap reference well, which is 3.2mm, and the actual position also tracks well with the position command, respectively. Under the position variation, the maximum displacement is under 100μm as shown in Fig. 12.

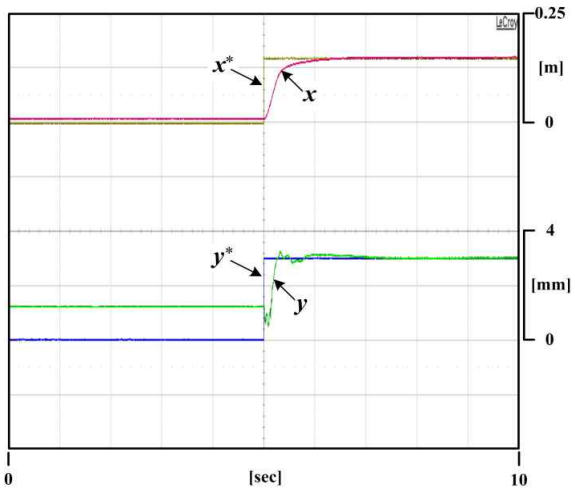

Fig. 11. Experimental waveform under air gap control (1.2mm~3.0mm) and position control (0.01m → 0.15m)

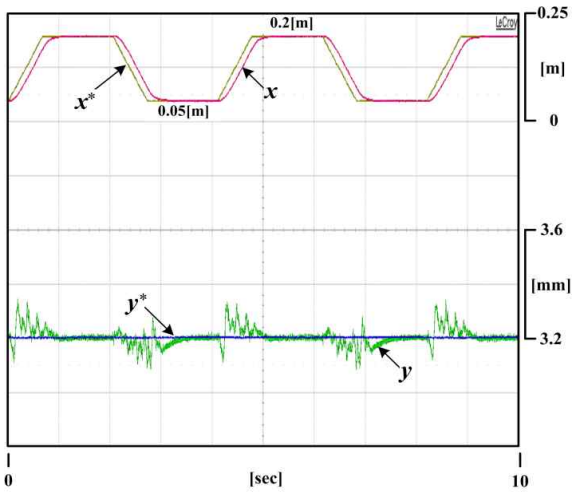

Fig. 12. Experimental waveform under air gap control (3.2mm) and position control (0.05m → 0.2m)

Fig. 13 represents the dynamic experimental results. When changing the mover position and air-gap command, the real mover position and air-gap are simultaneously controlled by the proposed coordinated current control as shown in Fig. 13.

From the various experimental results, the effectiveness of the proposed control algorithm based on the current phase shift control method and the transverse flux linear synchronous motor for magnetic levitation and position controls is verified.

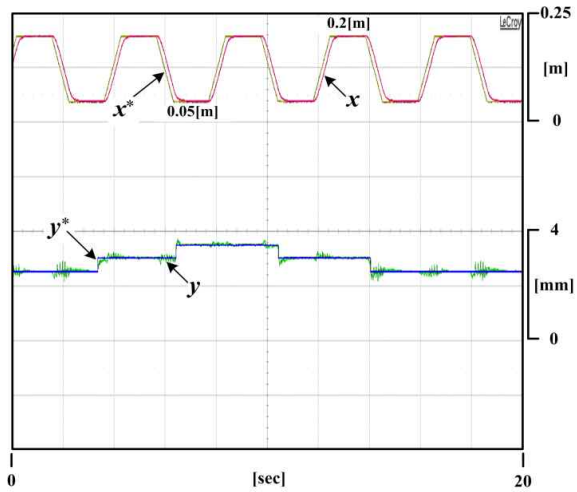

Fig. 13. Experimental waveform under air gap control (2.5mm~3.5mm) and position control (0.05m → 0.2m)

4. Conclusion

In this paper, the coordinated current control method for the normal force and thrust force of the IM-TFLSM based on the independent multi-phase winding, symmetric structures, and double-sided air-gap are proposed. In order to verify and realize the air-gap control based on the magnetic levitation and thrust control using coordinated control with the phase shifted current, a synchronous linear machine having the double-sided air-gap mover has been built and its control algorithm is performed. A simple PID gap controller with a practical derivative controller was applied for control of the normal force of the IM-TFLSM. In addition, the thrust and normal force can be controlled by the proposed method without any additional winding to generate the magnetic levitation unlike current conventional magnetic levitation systems. The effectiveness of the proposed control algorithm has been shown through several experimental results used in the prototype linear machine.

This research was partially supported by the Basic Science Research Program through the National Research Foundation of Korea (NRF) funded by the Ministry of Education, Science and Technology (No. 2013R1A1A1013670) and partially supported by the KERI grant funded by the Korea government(No. 14-12-N0101-82).

References

[1] J. de Boeij, E. A. Lomonova, A. J. A. Vandenput, "Optimization of contactless planar actuator with manipulator", IEEE Trans. Magn., vol. 44, pp. 1118-1121, 2008.
[2] D. H. Kang, "A study on the design of transverse flux linear motor with high power density", IEEE International Symposium on, vol. 2, pp. 707-711, Aug. 2002.
[3] A. Chiba, K. Sotome, Y. Iiyama, and M. A. Rahman, "A novel middle-point-current-injection-type bearingless PM synchronous motor for vibration suppression", IEEE Trans. Ind. Appl., vol. 47, no. 4, pp. 1700-1706, July/Aug. 2011.
[4] D. Bang, H. Polinder, J. A. Ferreira, and S. S. Hong, "Structural mass minimization of large direct-drive wind generators using a buoyant rotor structure", Energy Conversion Congress and Exposition, 2010 IEEE, pp. 3561-3568, Sept. 2010.
[5] S. H. Hwang, H. Li, J. W. Park, J. M. Kim, and D. J. Bang, "Vector control of multiple-module transverse flux PM generator for large-scale direct-drive wind turbines," Energy Conversion Congress and Exposition, 2011 IEEE, pp. 2365-2372, Sept. 2011.
[6] W. Y. Kim, J. M. Lee, and S. J. Kim, "Rolling motion control of a levitated mover in a permanent-magnet-type bearingless linear motor", IEEE Trans. Magn., vol. 46, no. 6, pp. 2482-2485, June 2010.
[7] W. G. Kim, S. J. Cho, "Control of transverse flux linear motor to the linear and curve section by using low-cost position sensors", Industrial Electronics, 2007. ISIE 2007 IEEE International Symposium on, pp. 1322-1326, Nov. 2007.
[8] V. Kluyskens, B. Dehez, and H. B. Ahmed, "Dynamical electromechanical model for magnetic bearings", IEEE Trans. Magn., vol. 43, no. 7, pp. 3287-3292, Jul. 2007.

Biography

Seon-Hwan Hwang

Seon-Hwan Hwang received his B.S., M.S., and Ph.D. degrees in Electrical Engineering from Pusan National University, Busan, Korea in 2004, 2006, and 2011, respectively. From 2011 to 2012, he was with the Center for Advanced Power Systems (CAPS), Florida State University, Tallahassee, FL, USA. Since 2012, he has been part of the Department of Electrical Engineering, Kyungnam University, Changwon, Korea. His current research interests include the control of electrical machines, power electronics, and wind power generation systems.

Soon-Kurl Kwon

Soon-Kurl Kwon received a Ph.D. degree in Electrical Engineering from Young-Nam University, Daegu, Korea. He joined the Department of Electrical Engineering, Kyungnam University, Changwon, Korea in 1983, in which he has served as a Professor. He was a Visiting Professor with the Virginia Polytechnic Institute and State University, Blacksburg in 1997. His research interests include application developments of power electronics circuits and systems.

Young-Gi Hwang

Young-Gi Hwang received his B.S. degree in Chemical Engineering from Pusan National University, Busan, Korea in 1974. He received M.S. and Ph.D. degrees in Chemical Engineering from Korea University, Korea in 1979 and 1986, respectively. From 1988 to 1989, he worked as a Postdoctoral Researcher in the University of Exeter, UK. He was a Visiting Professor with the University of Washington, Seattle in 1996. He is currently a Professor in the Department of Electrical Engineering, Kyungnam University, Changwon, Korea.

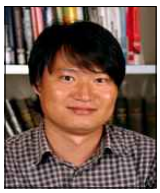

Deok-Je Bang

Deok-Je Bang received B.S. and M.S. degrees in Mechanical Engineering from Pukyong National University, Korea in 1996 and 1998, respectively. He received a Ph.D. degree in Electrical Engineering from the Delft University of Technology, The Netherlands, in 2010. From 1998 to 2006, he worked in the research area of electrical machines for Shinsung ENG Co. Ltd. In 2011, he was a Principal Researcher and Team Leader in the Wind Turbine Research Division, Hyundai Heavy Industries. Since 2012, he has been with the Korea Electrotechnology Research Institute, Changwon, Korea, where he is currently a Senior Researcher in the Electric Motor Research Center, Electric Propulsion Research Division. His current research interests include the design of large direct-drive generator systems for renewable energy.